Characterising a configuration interaction excited state using natural transition geminals

Characterising a configuration interaction excited state using natural transition geminals

J.P. Coe[a] & M.J. Paterson[a]

[a] Institute of Chemical Sciences, School of Engineering and Physical Sciences, Heriot-Watt University, Edinburgh, UK

PLEASE SCROLL DOWN FOR ARTICLE

Taylor & Francis
Taylor & Francis Group

INVITED ARTICLE

Characterising a configuration interaction excited state using natural transition geminals

J.P. Coe and M.J. Paterson[*]

Institute of Chemical Sciences, School of Engineering and Physical Sciences, Heriot-Watt University, Edinburgh, UK

We introduce natural transition geminals as a means to qualitatively understand a transition where double excitations are important. The first two A_1 singlet states of the CH cation are used as an initial example. We calculate these states with configuration interaction singles and state-averaged Monte Carlo configuration interaction (SA-MCCI). For each method, we compare the important natural transition geminals with the dominant natural transition orbitals. We then compare SA-MCCI and full configuration interaction with regards to the natural transition geminals using the beryllium atom. We compare using the natural transition geminals with analysing the important configurations in the CI expansion to give the dominant transition for the beryllium atom and the carbon dimer. Finally, we calculate the natural transition geminals for two electronic excitations of formamide.

1. Introduction

Using the important transitions from the ground state to characterise an excited state offers a qualitative interpretation of the excitation. Natural transition orbitals [1] have been shown to give a compact description of the important orbitals involved in an electronic excitation when modelled using single substitutions. For configuration interaction wave functions, however, double excitations may be dominant and these will not be detected when using natural transition orbitals. We, therefore, put forward the concept of natural transition geminals which will categorise the important two-electron transitions. As the one-particle transition density matrix may be calculated from the two-particle transition density matrix, then the natural geminals will also contain information regarding single-particle transitions. Therefore, they offer the possibility of a more general approach for characterising an electronic transition despite their added complexity and the difficulty in visualising a function of six coordinates.

Geminals, or antisymmetric two-electron functions, have been used in quantum chemistry methods since the 1950s and have a number of appealing features, see [2] for a review. However, these approaches perhaps did not become popular due to insufficient recovery of the correlation energy given their complexity. More recently, there have been promising improvements on these methods [3,4], and geminals have also been combined with explicitly correlated basis (F12) methods [5]. The natural geminals, defined as the two-electron eigenfunctions of the second-order reduced density matrix, were used to investigate the beryl-

lium atom in [6]. However, this paper represents the first application of natural transition geminals to our knowledge.

We test the approach of natural transition geminals on Monte Carlo configuration interaction (MCCI) [7,8] wave functions. MCCI allows a wave function, which can reproduce much of the full configuration interaction (FCI) results, to be built up using usually only a small fraction of the configurations that would be necessary for FCI. MCCI is an iterative scheme where the configuration space is stochastically enlarged, and configurations that have an absolute coefficient less than a certain value ($c_{\min}$) in the MCCI wave function are ultimately removed. The method has been employed to successfully find compact wave functions for excitations of atoms and small molecules [9], multipole moments, ionisation energies and electron affinities [10], and the potential curves of ground states [11]. We have recently used state-averaged MCCI [12] (SA-MCCI) to model excited potential curves with conical intersections or avoided crossings and the vertical excitations of small organic molecules. In this paper, we consider the ground and first singlet excited state of A_1 symmetry for the CH cation in the cc-pVDZ basis as an example to compare natural transition orbitals with natural transition geminals. We also contrast configuration interaction limited to single substitutions (CIS) and SA-MCCI on this system. We then compare the FCI natural transition geminals with those of SA-MCCI for the beryllium atom in the cc-pVDZ basis. We compare using the dominant configurations in the CI expansion with the natural transition geminals as a means to infer the main transition for an excitation of the beryllium

*Corresponding author. Email: M.J.Paterson@hw.ac.uk

atom and the carbon dimer. Finally, we calculate the natural transition geminals for two excitations of A' symmetry for formamide when using SA-MCCI and the def1-TZVP basis.

2. Methods

2.1. Monte Carlo configuration interaction

In this work, we use MCCI [7,8] with a form of state averaging (SA-MCCI) and employ Slater determinants (SDs). We briefly describe the iterative scheme which begins with a Hartree–Fock SD. SA-MCCI augments a set of SDs randomly with single and double substitutions which maintain the symmetry of the wave function. The Hamiltonian matrix is then constructed and diagonalised to give the first s states. We then create state-averaged coefficients using $c_i = \sum_{j=1}^{s} |c_{i,j}|$, and SDs that have just been included are removed if $|c_i| < c_{\min}$ [12]. This approach is repeated and every 10 iterations, all SDs become candidates for removal.

2.2. Natural transition orbitals

The natural transition orbitals [1] are found by performing a singular value decomposition on the single-particle transition density matrix which, in spatial-spin coordinates, is

$$T(\vec{x}_A, \vec{x}_B) = N \int \Psi_2^*(\vec{x}_A, \vec{x}_2, \ldots, \vec{x}_N) \times \Psi_1(\vec{x}_B, \vec{x}_2, \ldots, \vec{x}_N) d\vec{x}_2, \ldots, \vec{x}_N. \quad (1)$$

For two N electron wave functions constructed from SDs and the same set of molecular orbitals (MOs) ($\phi_1 - \phi_M$), we can write the single-particle transition density matrix in terms of the spin orbitals ($\chi_1 - \chi_{2M}$):

$$T(\vec{x}_A, \vec{x}_B) = \sum_{i=1}^{2M} \sum_{j=1}^{2M} \chi_i^*(\vec{x}_A) T_{ij} \chi_j(\vec{x}_B). \quad (2)$$

The SDs comprising the wave functions must have no more than one difference to contribute to T, so we have

$$T_{ij} = \langle \Psi_2| c_i^\dagger c_j |\Psi_1 \rangle, \quad (3)$$

where i and j range over all spin orbitals. If we consider a ground state where all spatial orbitals are doubly occupied and a triplet state formed from a single spatial orbital replacement, then the contributions to T would cancel if we were to sum over spins. Therefore, we do not average over spins here. Empty rows and columns in T may be removed and the matrix relabelled followed by a singular value decomposition $T = U D V^\dagger$ to give the natural transition orbitals and their eigenvalues for Ψ_2 and Ψ_1.

We may build the single-particle transition density matrix for two MCCI wave functions, $\Psi_2 = \sum_i c_i \text{SD}_i$ and $\Psi_1 = \sum_j d_j \text{SD}_j$, by noting that SDs i and j in maximum coincidence only contribute if there is one difference with orbitals k and l responsible,

$$T_{kl} \rightarrow T_{kl} + e_p c_i^* d_j, \quad (4)$$

or no differences,

$$T_{mm} \rightarrow T_{mm} + e_p c_i^* d_j. \quad (5)$$

Here m runs over all spin orbitals in either SD and e_p is the sign from placing the SDs in maximum coincidence.

2.3. Natural transition geminals

We construct natural transition geminals by first considering the two-particle transition density matrix:

$$T^{(2)}(\vec{x}_A, \vec{x}_{A'}, \vec{x}_B, \vec{x}_{B'}) = \frac{N(N-1)}{2} \int \Psi_2^*(\vec{x}_A, \vec{x}_{A'}, \vec{x}_3, \ldots, \vec{x}_N) \times \Psi_1(\vec{x}_B, \vec{x}_{B'}, \vec{x}_3, \ldots, \vec{x}_N) d\vec{x}_3, \ldots, \vec{x}_N, \quad (6)$$

which can be written as

$$T^{(2)}(\vec{x}_A, \vec{x}_{A'}, \vec{x}_B, \vec{x}_{B'}) = \sum_{i=1}^{M_G} \sum_{j=1}^{M_G} G_i^*(\vec{x}_A, \vec{x}_{A'}) T_{ij}^{(2)} G_j(\vec{x}_B, \vec{x}_{B'}), \quad (7)$$

where G_i are the $\binom{2M}{2} = M_G$ unique geminals formed from pairs of spin orbitals. For example,

$$G_1(\vec{x}_1, \vec{x}_2) = |1, \bar{2}\rangle. \quad (8)$$

Here the ket at the right-hand side is a normalised SD and the 1 without a bar represents ϕ_1 with an up spin, while with a bar it would have a down spin.

The two-particle transition matrix in terms of geminals can be constructed as

$$T_{ij}^{(2)} = \langle \Psi_2| c_{i_1}^\dagger c_{i_2}^\dagger c_{j_1} c_{j_2} |\Psi_1 \rangle. \quad (9)$$

Here we label the spin orbitals with spin up using the MO number (1–M) while the spin-down MOs are labelled from $M+1$ to $2M$ using the MO number plus M. We stipulate that $i_1 < i_2$ and $j_1 < j_2$ for our list of unique geminals which we map from two labels to one using

$$i(i_1, i_2) = 2(i_1 - 1)M + i_2 - i_1 - \frac{(i_1 - 1)i_1}{2}. \quad (10)$$

Table 1. Example of labelling for geminals when using two molecular orbitals.

Geminal	i_1	i_2	i
$\lvert 1, 2 \rangle$	1	2	1
$\lvert 1, \bar{1} \rangle$	1	3	2
$\lvert 1, \bar{2} \rangle$	1	4	3
$\lvert 2, \bar{1} \rangle$	2	3	4
$\lvert 2, \bar{2} \rangle$	2	4	5
$\lvert \bar{1}, \bar{2} \rangle$	3	4	6

An example of the geminal labelling scheme for two MOs is given in Table 1.

Similarly to the procedure for the natural transition orbitals, we remove empty rows and columns from $\boldsymbol{T^{(2)}}$, then perform a singular value decomposition to give the natural transition geminals for the two states.

We construct the two-particle transition matrix by considering all SDs that comprise the two wave functions: $\Psi_2 = \sum_i c_i \mathrm{SD}_i$ and $\Psi_1 = \sum_j d_j \mathrm{SD}_j$. We note that now SD_i and SD_j only contribute if they have two or fewer differences when in maximum coincidence.

If the two differences, in order of occurrence, in SD_i are the spin orbitals k_1 and k_2, while in SD_j, they are l_1 and l_2. Then, we have

$$T_{kl} \rightarrow T_{kl} + e_g e_p c_i^* d_j, \qquad (11)$$

where e_p is the sign from placing the SDs in maximum coincidence and e_g the sign from changing the order of k_1 and k_2 so that $k_1 < k_2$, and similarly for l_1 and l_2 which are then mapped to k and l.

For one difference caused by spin orbitals k_1 and l_1 in SD_i and SD_j, respectively, then $k_2 = l_2$ ranges over all the other spin orbitals in the SD and the order of, for example, k_1 and k_2 is swapped if k_2 occurs before k_1 in the reordered SD. This results in $N - 1$ contributions which, when the labels are mapped to k and l, are of the form,

$$T_{kl} \rightarrow T_{kl} + e_g e_p c_i^* d_j. \qquad (12)$$

Finally, we have the case of no differences. This results in

$$T_{mm} \rightarrow T_{mm} + e_p c_i^* d_j, \qquad (13)$$

where m ranges over all $\binom{N}{2}$ possible geminals which can be constructed from the spin orbitals of either of the SDs.

3. CH cation

As an example of the use of natural transition geminals, we now look at the ground and first singlet excited states of A_1 symmetry of the CH cation at a bond length of

1.13 Å. We use one frozen orbital for the CI calculations. We analyse the CIS, then the MCCI wave functions when using the cc-pVDZ basis. The Hartree–Fock HOMO and LUMO, when plotted with Molden [13] using a 0.1 cut-off value, are displayed in Figure 1 where the carbon atom is at the front.

3.1. Natural transition orbitals

When using SDs, a CIS calculation gives the first excited state as a triplet here. The second excited state has an energy of -37.38 hartree, which agrees with the Molpro [14] result using configuration state functions (CSFs) of -37.38, so would be expected to be a singlet. For the natural transition orbitals, we find that the main spin-up and spin-down transitions are the same with eigenvalue 0.71 while the next transition has 3.8×10^{-2} for both spins and the other eigenvalues are negligible. In the following results, we neglect MOs with less than 10^{-1} contribution to the natural transition orbitals. The strongest transition is essentially $\phi_3 \rightarrow 0.99\phi_4 + 0.12\phi_7$. This is then the HOMO to mainly the next orbital of A_1 symmetry. The next transition is more complicated but is approximately $\phi_2 \rightarrow 0.11\phi_4 + 0.64\phi_5 - 0.70\phi_7 - 0.25\phi_9 + 0.18\phi_{10}$.

The SA-MCCI calculation with $c_{\min} = 5 \times 10^{-4}$ was run for 100 iterations on four processors. This gave -38.00 and -37.75 hartree for the ground and excited states, respectively. These energies agree to two decimal places with the FCI results using PSI3 [15] although the 1387 SDs used by SA-MCCI represent a large fraction of the small FCI space of 6129 SDs.

Now the three main spin-up and spin-down transitions have eigenvalues of 7×10^{-2} for the first two spin pairs and 4×10^{-2} for the third pair, while the others are less than 6×10^{-4}. Each up-spin transition has the same relative phase as the down spin for each of these three confirming that the excited state is not a triplet. The first two transitions are

$$0.94\phi_{11} - 0.20\phi_{12} - 0.25\phi_{13} + 0.16\phi_{14}$$
$$\rightarrow -0.99\phi_{11} + 0.15\phi_{12},$$

$$-0.94\phi_{15} + 0.20\phi_{16} + 0.25\phi_{17} - 0.16\phi_{18}$$
$$\rightarrow -0.99\phi_{15} + 0.15\phi_{16},$$

while the third is $0.22\phi_2 + 0.97\phi_3 \rightarrow \phi_8$.

With the MCCI wave function approaching the FCI, here we see that excitations to the LUMO states are now some of the main transitions, but they are not from the HOMO as the symmetry must be preserved. Similarly, one of the main transitions is from the HOMO, but it is not to the LUMO states. However, the natural transition orbitals only consider single excitations, so we now compare these results with the natural transition geminals.
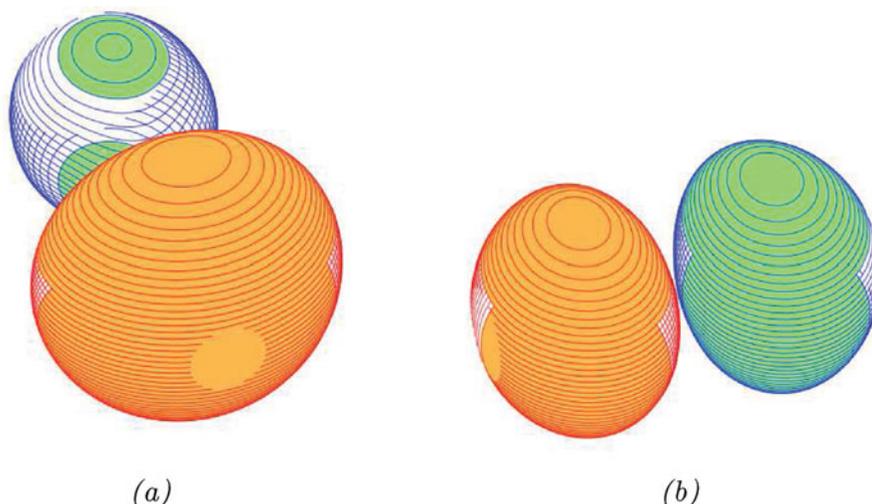
Figure 1. (a) HOMO ϕ_3 of A_1 symmetry; (b) LUMOs are ϕ_{11} and ϕ_{15} of B_1 and B_2 symmetries, respectively. Other LUMO is the same as that depicted but for a 90°-clockwise rotation along the CH bond.

3.2. Natural transition geminals

In the following results, we neglect geminals that contribute less than 10^{-1} to the natural transition geminals. When modelling the system using CIS and using natural transition geminals, we find a transition with eigenvalue 0.999: $|3, \bar{3}\rangle \rightarrow 0.70|3, \bar{4}\rangle + 0.70|4, \bar{3}\rangle$.

There are then four with eigenvalue 0.71:

$$|3, \bar{2}\rangle \rightarrow 0.99|4, \bar{2}\rangle + 0.12|7, \bar{2}\rangle,$$
$$|2, 3\rangle \rightarrow 0.99|2, 4\rangle + 0.12|2, 7\rangle,$$
$$|2, \bar{3}\rangle \rightarrow 0.99|2, \bar{4}\rangle + 0.12|2, \bar{7}\rangle,$$
$$|\bar{2}, \bar{3}\rangle \rightarrow 0.99|\bar{2}, \bar{4}\rangle + 0.12|\bar{2}, \bar{7}\rangle.$$

Then, there is one with eigenvalue 5.4×10^{-2}: $|2, \bar{2}\rangle \rightarrow 0.45|2, \bar{5}\rangle - 0.49|2, \bar{7}\rangle - 0.17|2, \bar{9}\rangle + 0.13|2, \bar{10}\rangle + (|i, \bar{j}\rangle \leftrightarrow |j, \bar{i}\rangle)$, while the rest are negligible. We see that the ϕ_3 to ϕ_4 with some ϕ_7 is the main single-particle transition similar to the results using natural transition orbitals.

For the SA-MCCI wave functions, the main eigenvalue for the natural transition geminals is 0.96, while all the other eigenvalues are less than 9.63×10^{-2}. The dominant transition is now revealed as a double excitation which is mainly composed of the two HOMO electrons being excited to doubly occupied LUMOs:

$$0.13|2, \bar{2}\rangle - 0.97|3, \bar{3}\rangle$$
$$\rightarrow -0.69|11, \bar{1}1\rangle + 0.1|11, \bar{1}2\rangle + 0.1|12, \bar{1}1\rangle$$
$$+ 0.69|15, \bar{1}5\rangle - 0.1|15, \bar{1}6\rangle - 0.1|16, \bar{1}5\rangle.$$

4. Beryllium atom

We now compare the SA-MCCI natural transition geminals with those of FCI for the electronic excitation between the first two A_g singlet states in the beryllium atom using a cc-pVDZ basis. We use no frozen orbitals and D_{2h} symmetry. A cut-off of $c_{min} = 5 \times 10^{-3}$ is employed for the SA-MCCI calculation. The Hartree–Fock orbitals have ϕ_2 as the HOMO, while the LUMOs are ϕ_6, ϕ_8, and ϕ_{11}. The FCI result used 1093 SDs to give an excitation energy of 7.75 eV. We find that there is a transition with eigenvalue 1, four with 0.15, four with 0.12, and four with 0.11, while the rest have eigenvalues lower than 0.02. The largest eigenvalue corresponds to the transition:

$$-0.95|2, \bar{2}\rangle + 0.14|6, \bar{6}\rangle + 0.14|8, \bar{8}\rangle + 0.14|11, \bar{1}1\rangle$$
$$\rightarrow 0.14|2, \bar{4}\rangle + 0.14|4, \bar{2}\rangle + 0.58|6, \bar{6}\rangle + 0.18|6, \bar{7}\rangle$$
$$+ 0.18|7, \bar{6}\rangle - 0.67|11, \bar{1}1\rangle - 0.21|11, \bar{1}2\rangle$$
$$- 0.21|12, \bar{1}1\rangle.$$

For the SA-MCCI results, we used 100 iterations and four processors. This gave an excitation energy of 7.76 eV using 27 SDs. The eigenvalues for the natural transition geminals are similar to the FCI results: one transition with eigenvalue 1, four with 0.15, four with 0.13, and four with 0.10, while the rest have eigenvalues lower than 0.03.

The largest eigenvalue corresponds to the transition:

$$-0.95|2, \bar{2}\rangle + 0.14|6, \bar{6}\rangle + 0.14|8, \bar{8}\rangle + 0.14|11, \bar{1}1\rangle$$
$$\rightarrow 0.12|2, \bar{4}\rangle - 0.10|2, \bar{5}\rangle + 0.12|4, \bar{2}\rangle - 0.10|5, \bar{2}\rangle$$
$$+ 0.69|6, \bar{6}\rangle + 0.22|6, \bar{7}\rangle + 0.22|7, \bar{6}\rangle - 0.14|8, \bar{8}\rangle$$
$$- 0.55|11, \bar{1}1\rangle - 0.17|11, \bar{1}2\rangle - 0.17|12, \bar{1}1\rangle.$$

We see that when ignoring geminals with coefficient less than 0.1, then the ground-state natural transition geminals are the same for FCI and SA-MCCI with a reasonably large cut-off. The excited-state natural transition geminals have slightly different coefficients when using SA-MCCI and, notably, geminals with ϕ_5 and ϕ_8 are present in the

SA-MCCI results but do not have a large enough coefficient in the FCI results to be displayed. The transition cannot be straightforwardly described as involving a double excitation of MOs as the LUMOs also occur as doubly occupied geminals in the ground state albeit with small coefficients. By considering the largest contributions, however, we can approximately describe the transition as comprising mainly a double excitation from the doubly occupied HOMO to the doubly occupied LUMOs of B_{1u} and B_{3u} symmetries.

For the beryllium atom, we also consider if the coefficients in the FCI expansion will reveal similar information about the important transition when using the natural orbitals of the ground state. For the natural transition geminals, we find that the eigenvalues are approximately the same as when using the Hartree–Fock MOs. The transition corresponding to the largest eigenvalue is

$$0.95|2, \bar{2}\rangle - 0.17|6, \bar{6}\rangle - 0.17|8, \bar{8}\rangle - 0.17|11, \bar{1}1\rangle$$
$$\rightarrow -0.11|2, \bar{4}\rangle - 0.11|2, \bar{5}\rangle - 0.11|4, \bar{2}\rangle - 0.11|5, \bar{2}\rangle$$
$$+ 0.18|6, \bar{6}\rangle - 0.74|8, \bar{8}\rangle + 0.13|8, \bar{9}\rangle + 0.13|9, \bar{8}\rangle$$
$$+ 0.56|11, \bar{1}1\rangle.$$

We see that due to the use of the ground-state natural orbitals, the coefficients are different particularly for some of the doubly occupied orbitals in the excited state.

Ordering the SDs in the FCI wave function by absolute coefficient gives for the ground state:

$$\Psi_0 = 0.95|1, \bar{1}, 2, \bar{2}\rangle - 0.17|1, \bar{1}, 11, \bar{1}1\rangle$$
$$- 0.17|1, \bar{1}, 8, \bar{8}\rangle - 0.17|1, \bar{1}, 6, \bar{6}\rangle + \cdots,$$

while for the excited, we have

$$\Psi_1 = -0.74|1, \bar{1}, 8, \bar{8}\rangle + 0.56|1, \bar{1}, 11, \bar{1}1\rangle$$
$$+ 0.18|1, \bar{1}, 6, \bar{6}\rangle + \cdots.$$

In this case, one can deduce by inspection of the wave functions the main transition in the excitation and this is in agreement with the natural transition geminal result to two decimal places. Due to ϕ_1 being doubly occupied in each of the main configurations, then this becomes essentially a two-particle system, so it may be much more challenging to find by eye the constituents of the main transition in larger systems without recourse to the natural transition geminals.

5. Carbon dimer

We now compare the natural transition geminals with the important configurations in a CI expansion for the carbon dimer. Here we use a bond length of 2.348 Bohr, the 6-31G* basis, and a cut-off of $c_{\min} = 5 \times 10^{-3}$, for an SA-MCCI calculation. The Hartree–Fock MOs are used as the system is sufficiently large that it is too computationally challenging to find the FCI natural orbitals. We freeze orbitals 1 and

15, hence they do not appear in any of the following expansions. We calculate the ground and first excited states using 100 iterations on four processors. The largest eigenvalue for the natural transition geminals is 0.92, while the rest are less than 0.12. The corresponding transition is

$$0.97|11, \bar{1}1\rangle - 0.15|8, \bar{8}\rangle - 0.13|16, \bar{1}6\rangle$$
$$- 0.11|25, \bar{2}5\rangle \rightarrow 0.92|3, \bar{3}\rangle - 0.34|16, \bar{1}6\rangle.$$

When sorting the CI expansions by the absolute value of the coefficient, we find the following for the ground state:

$$\Psi_0 = 0.86|2, \bar{2}, 8, \bar{8}, 11, \bar{1}1, 16, \bar{1}6\rangle$$
$$- 0.33|2, \bar{2}, 3, \bar{3}, 8, \bar{8}, 11, \bar{1}1\rangle + \cdots$$

and for the excited state, we see that

$$\Psi_1 = 0.92|2, \bar{2}, 3, \bar{3}, 8, \bar{8}, 16, \bar{1}6\rangle$$
$$- 0.17|2, \bar{2}, 3, \bar{3}, 8, \bar{8}, 11, \bar{1}1\rangle$$
$$- 0.14|2, \bar{2}, 3, \bar{3}, 11, \bar{1}1, 16, \bar{1}6\rangle + \cdots.$$

Here it is not so straightforward to identify the dominant transition from the CI expansion and this would be expected to become more challenging if larger numbers of particles are considered.

6. Formamide

Finally, we look at the $1\,^1A' \rightarrow 2\,^1A'$ transition of formamide. We use SA-MCCI running on 12 processors for 50 iterations with a cut-off of $c_{\min} = 5 \times 10^{-4}$. The def1-TZVP basis [16] is used and three core orbitals are frozen. We use the MP2/6-31G* optimised geometry of [17]. The Hartree–Fock results give the HOMO as ϕ_{59}, which is the second orbital of A'' symmetry, while the LUMO is ϕ_{11}. We find the excitation energy to the first excited state to be 6.1 eV here using 48, 832 SDs compared with an FCI space of around 10^{21} SDs. In [17], a CASPT2 result was 7.44 eV, while the CCSD response result appeared too low at 4.52 eV. The natural transition geminals for the first excited state have 1 eigenvalue of 0.95 and 44 of around 0.67, then the rest are less than 0.07. The transition corresponding to the largest eigenvalue is

$$0.99|59, \bar{5}9\rangle \rightarrow 0.69|59, \bar{6}0\rangle - 0.69|60, \bar{5}9\rangle.$$

This suggests that the transition is a singlet to triplet, so we look at the next excited state. We now find an excitation energy of 8.4 eV and the natural transition geminals now have 1 eigenvalue of 0.91, 44 of ~0.6, 5 around 0.1, and the rest less than 0.1. The largest eigenvalue is for the transition:

$$0.99|59, \bar{5}9\rangle \rightarrow 0.70|59, \bar{6}0\rangle + 0.69|60, \bar{5}9\rangle,$$

where we can see now that it is almost a singlet to singlet although there is a small amount of spin contamination.

The second largest eigenvalue of 0.67 corresponds to the transition:

$$0.66|59, \bar{58}\rangle + 0.75|58, \bar{59}\rangle$$
$$\rightarrow -0.22|60, \bar{60}\rangle + 0.63|60, \bar{58}\rangle - 0.1|58, \bar{61}\rangle$$
$$- 0.09|61, \bar{58}\rangle + 0.72|58, \bar{60}\rangle.$$

Here we have included the $|61, \bar{58}\rangle$ geminal despite its coefficient being lower than 0.1 to show that the excitation is approximately singlet to singlet although this natural transition geminal seems to suggest slightly more spin contamination. The large number of non-negligible eigenvalues here makes it difficult to discuss what constitutes the main transition. However, the results suggest that when modelled with SA-MCCI using SDs and a cut-off of $c_{min} = 5 \times 10^{-4}$, then the transition to the first excited singlet state of formamide of A' symmetry with largest eigenvalue can be approximately thought of as a single excitation from the HOMO ϕ_{59} to ϕ_{60} although there is a small amount of double excitation character in the natural transition geminals of the second largest eigenvalue.

7. Summary

In this paper, we introduced the use of natural transition geminals to aid in understanding excited states of configuration interaction wave functions that contain double excitations from the ground state. We used the ground and first excited singlets of the CH cation as an initial example which we modelled using CIS and SA-MCCI. The SA-MCCI results agreed with the FCI energies to two decimal places. Natural transition orbitals revealed that the excited state when using CIS could be essentially described as the HOMO (ϕ_3) being excited to ϕ_4 with some ϕ_7. Natural transition geminals were then seen to reproduce this information. For the SA-MCCI wave functions, natural transition orbitals allowed the LUMOs (ϕ_{11} and ϕ_{15}) to be viewed as some of the main orbitals created in the excited wave function during the transition but these came from the replacement of other orbitals of B_1 or B_2 symmetry. This is due to the excitations being symmetry preserving so a double excitation would be needed to allow A_1 orbitals to be replaced with B_1. Natural transition geminals then allowed the dominant transition for the SA-MCCI wave functions to be seen as a double excitation from mainly the doubly occupied HOMOs to doubly occupied LUMOs.

We saw that the FCI and SA-MCCI natural transition geminals were similar for the first singlet excitation of the beryllium atom when using the cc-pVDZ basis. Here the SA-MCCI result used 27 SDs compared with 1093 in the FCI calculation. Some geminals were not important enough to be in the FCI result yet were in the SA-MCCI result; however, the natural transition geminals showed that the transition was approximately dominated by a double excitation from the HOMO to two of the LUMOs in both cases even though the transition was somewhat complicated. When using ground-state natural orbitals, we compared the transition suggested by the important configurations in the FCI expansions with the natural transition geminals and found for this system that they agreed. We then considered the carbon dimer and saw that it was more difficult to identify the important transition by looking at the CI expansion for this larger system.

The natural transition geminals allowed us to identify the first excited state of formamide as a triplet when using SA-MCCI with SDs. The second excited state of A' symmetry appeared to be approximately a singlet, although some spin contamination was observed in the natural transition geminals, and there was a large number of significant eigenvalues suggesting that there may not be a simple interpretation of the transition. The two largest eigenvalues had a single-particle excitation from the HOMO to another orbital of the same symmetry as the main contribution here although the transition for the second largest eigenvalue had some double excitation character.

Due to the number of geminals scaling as $O(M^2)$, where M is the number of orbitals, calculating the natural transition geminals by performing a singular value decomposition can become onerous as the size of the basis becomes large, although we note that natural transition geminals could be used for most complete active space self-consistent field (CASSCF) wave functions due to the restriction on the number of orbitals in the active space. Furthermore, as mentioned in Section 1, the use of geminals is more complicated than orbitals and we do not know of a useful approach to visualise the natural transition geminals. Despite these difficulties, it appears that the natural transition geminals can be useful for giving a qualitative understanding of the main transitions to excited states where single and double excitations are important when using configuration interaction wave functions.

References

[1] R.L. Martin, J. Chem. Phys. **118**, 4775 (2003).
[2] P.R. Surján, in *Topics in Current Chemistry*, Vol. 203, edited by P.R. Surján (Springer Verlag, Berlin, 1999), pp. 63–88.
[3] V.A. Rassolov, J. Chem. Phys. **117**, 5978 (2002).
[4] V.A. Rassolov, F. Xu, and S. Garashchuk, J. Chem. Phys. **120**, 10385 (2004).
[5] E.F. Valeev, J. Chem. Phys. **125**, 244106 (2006).
[6] D.W. Smith and S.J. Fogel, J. Chem. Phys. **43** (10), S91–S96 (1965).

[7] J.C. Greer, J. Comput. Phys. **146**, 181 (1998).

[8] L. Tong, M. Nolan, T. Cheng, and J.C. Greer, Comput. Phys. Commun. **131**, 142 (2000).

[9] W. Győrffy, R.J. Bartlett, and J.C. Greer, J. Chem. Phys. **129**, 064103 (2008).

[10] J.P. Coe, D.J. Taylor, and M.J. Paterson, J. Comput. Chem. **34**, 1083 (2013).

[11] J.P. Coe, D.J. Taylor, and M.J. Paterson, J. Chem. Phys. **137**, 194111 (2012).

[12] J.P. Coe and M.J. Paterson, J. Chem. Phys. **139**, 154103 (2013).

[13] G. Schaftenaar and J.H. Noordik, J. Comput. Aided Mol. Design **14**, 123 (2000).

[14] H.J. Werner, P.J. Knowles, G. Knizia, F.R. Manby, M. Schütz, P. Celani, T. Korona, R. Lindh, A. Mitrushenkov, G. Rauhut, K.R. Shamasundar, T.B. Adler, R.D. Amos, A. Bernhardsson, A. Berning, D.L. Cooper, M.J.O. Deegan, A.J. Dobbyn, F. Eckert, E. Goll, C. Hampel, A. Hesselmann, G. Hetzer, T. Hrenar, G. Jansen, C. Köppl, Y. Liu, A.W. Lloyd, R.A. Mata, A.J. May, S.J. McNicholas, W. Meyer, M.E. Mura, A. Nicklass, D.P. O'Neill, P. Palmieri, K. Pflüger, R. Pitzer, M. Reiher, T. Shiozaki, H. Stoll, A.J. Stone, R. Tarroni, T. Thorsteinsson, M. Wang, and A. Wolf, Molpro, version 2010.1, a package of ab initio programs (Cardiff, 2010). http://www.molpro.net.

[15] T.D. Crawford, C.D. Sherrill, E.F. Valeev, J.T. Fermann, R.A. King, M.L. Leininger, S.T. Brown, C.L. Janssen, E.T. Seidl, J.P. Kenny, and W.D. Allen, J. Comput. Chem. **28**, 1610 (2007).

[16] A. Schäfer, H. Horn, and R. Ahlrichs, J. Chem. Phys. **97**, 2571 (1992).

[17] M. Schreiber, M.R. Silva-Junior, S.P.A. Sauer, and W. Thiel, J. Chem. Phys. **128**, 134110 (2008).